

# Pressure-induced structural, electronic, and magnetic effects in BiFeO<sub>3</sub>

O. E. González-Vázquez and Jorge Íñiguez

*Institut de Ciència de Materials de Barcelona (ICMAB-CSIC), Campus UAB, 08193 Bellaterra, Spain*

(Received 5 October 2008; published 5 February 2009)

We present a first-principles study of multiferroic BiFeO<sub>3</sub> at high pressures. Our work reveals the main structural (change in Bi's coordination and suppression of the ferroelectric distortion), electronic (spin crossover and metallization), and magnetic (loss of order) effects favored by compression and how they are connected. Our results are consistent with the striking manifold transition observed experimentally by Gavriluk *et al.* [Phys. Rev. B 77, 155112 (2008)] and provide an explanation for it.

DOI: [10.1103/PhysRevB.79.064102](https://doi.org/10.1103/PhysRevB.79.064102)

PACS number(s): 64.70.K-, 71.15.Mb, 75.30.Wx, 75.80.+q

## I. INTRODUCTION

Room-temperature multiferroic BiFeO<sub>3</sub> (BFO) is one of the most intensively studied materials of the moment. BFO is among the most promising multiferroics from the applications perspective, and the latest results regarding its fundamental properties<sup>1</sup> and the engineering possibilities it offers<sup>2,3</sup> continue to fuel the interest in it.

Indeed, recent works suggest the correlations between the structural, electronic, and magnetic properties of BiFeO<sub>3</sub> are not understood yet. We have evidence for a large sensitivity of BFO's conductivity to magnetic order,<sup>1,4</sup> a metal-insulator (MI) transition driven by structural changes at high temperatures,<sup>5</sup> high conductivity at ferroelectric domain walls,<sup>6</sup> and even a spin-glass phase below 150 K.<sup>7</sup> Yet, the results most revealing of the complex interactions in BFO may be those of Gavriluk *et al.*<sup>8,9</sup> These authors observed a pressure-driven diffuse transition, occurring at room temperature in the 40–50 GPa range, that involves a structural change, loss of magnetic order, and metallization. The driving force behind such transformations, tentatively attributed to a spin crossover of Fe<sup>3+</sup>, remains to be clarified.

Here we report on a first-principles study of the high-pressure behavior of BFO in the limit of very low temperatures (nominally, 0 K). Our results reproduce the essential observations of Gavriluk *et al.*, thus revealing the mechanisms that can lead to a manifold (structural/electronic/magnetic) transition in this material.

## II. METHODOLOGY

We used the local-density approximation (LDA) (Ref. 10) to density-functional theory as implemented in the Vienna *ab-initio* simulation package (VASP),<sup>11</sup> including the so-called LDA+*U* correction of Dudarev *et al.*<sup>12</sup> for a better treatment of iron's 3*d* electrons. We used the projector-augmented wave (PAW) scheme,<sup>13</sup> solving for the following electrons: Fe's 3*d* and 4*s*, Bi's 6*s* and 6*p*, and O's 2*s* and 2*p*. The electronic wave functions were described with a plane-wave basis truncated at 400 eV, and we used a  $\Gamma$ -centered  $7 \times 7 \times 7$  *k*-point grid for Brillouin-zone integrations. These calculation conditions were checked to render converged results and to reproduce published first-principles data for BFO at 0 GPa.<sup>4,14</sup> The technicalities of our calculations are thus standard, but our use of the LDA+*U* asks for a comment: In this

work we compared the energies of different electronic phases (insulating/metallic) in which the Fe<sup>3+</sup> ions display different spin states. Doing this accurately constitutes a challenge for any *ab-initio* approach; in particular, while commonly used to study such problems, the computationally efficient LDA+*U* should be employed with caution in this context. For this reason, we repeated all our calculations for different values of the *U* parameter in the 0–4 eV range, and thus made sure our qualitative conclusions are reliable. (Unless otherwise indicated, the reported results are for *U*=3 eV.)

Phase transitions in BFO under moderately high pressures have already been studied theoretically.<sup>4</sup> In this work, however, we were not interested in the relatively *mild* effects so far investigated. Rather, we wanted to determine whether pressure may induce profound changes in the electronic structure of the compound. Thus, we restricted our simulations to the 10-atom cell of the *R3c* phase of BFO stable at ambient conditions (see inset in Fig. 1), assuming this is representative enough to capture the phenomena of interest. Then, as a function of volume (i.e., pressure), we performed structural relaxations for a variety of atomic, electronic, and magnetic configurations. That allowed us to identify a large number of possible phases and determine their relative stability and properties. All the structural relaxations were started from a nonsymmetric atomic configuration (corre-

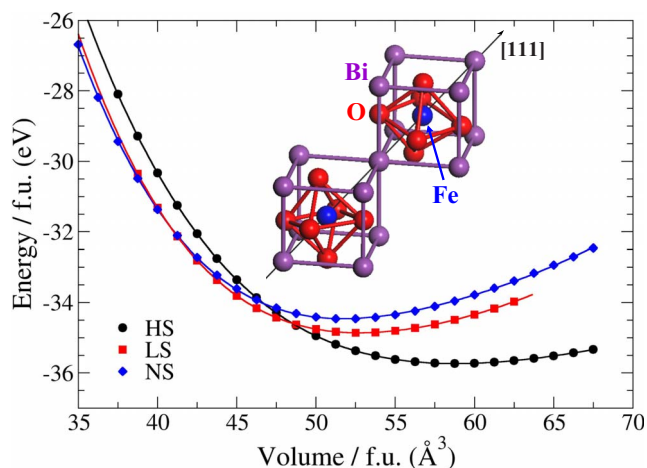


FIG. 1. (Color online).  $E(V)$  curves for the BFO phases here considered (see text). Inset: structure of the ferroelectric *R3c* phase of BFO stable at ambient conditions.

sponding to the  $P1$  space group) so that the material is allowed to find its lowest-energy state. Further, noting that the structures obtained from our structural relaxations were usually highly symmetric (with  $R3c$  and  $R\bar{3}c$  space groups, typically), we ran structural stability checks in a few selected cases (e.g., for the “LS phase” discussed below at about 36 GPa and about 65 GPa) and ratified that the obtained solutions are stable against symmetry-lowering distortions. Different electronic configurations (e.g., high- and low-spin states of the  $\text{Fe}^{3+}$  cations) were achieved in the calculations by appropriately choosing the starting spin state. As done in other first-principles studies,<sup>14,15</sup> we neglected the long-period spin cycloid in BFO.

Hence, the adopted methodology relies on substantial simplifications as regards the treatment of the strong correlation effects (described at the LDA+ $U$  level) and the possible atomic and magnetic structures that  $\text{BiFeO}_3$  can adopt under compression (since we only considered a particular 10-atom cell). Accordingly, this work should be considered as a first step in the study of a very complex problem on which our experimental knowledge is currently limited. Our conclusions are thus qualitative in nature, and pertain only to the main most drastic electronic and structural effects favored by pressure.

### III. RESULTS

#### A. Structural and spin transitions

Figure 1 displays our results for the equation of state of the BFO phases we found to be stable in some pressure range. The obtained pressure-driven transitions are better visualized in Fig. 2, which shows the pressure dependence of the key properties. At ambient and moderately high pressures we obtained the usual ferroelectric  $R3c$  phase of BFO, with  $G$ -type antiferromagnetic (AFM) order and  $\text{Fe}^{3+}$  in a high-spin (HS) state. Then, we found that at about 36 GPa BFO undergoes a first-order phase transition to a phase with the  $\text{Fe}^{3+}$  ions in a low-spin (LS) configuration. The concurrent drops in volume and iron’s magnetic moment across the HS-LS transition can be seen, respectively, in Figs. 2(b) and 2(c). (The magnetic moments are nearly pressure-independent within both the HS and LS phases.) Finally, a metallic phase with no localized magnetic moments, denoted as “NS phase,” where NS stands for “no spin,” becomes stable above 72 GPa. Such a paramagnetic metallic phase is typical of transition-metal oxides at high pressures.<sup>16</sup>

The atomic structure of the obtained stable phases is fully specified in Fig. 3, which shows the pressure dependence of the unit cell and the structural parameters associated to the occupied Wyckoff orbits as defined in Table I. (All the stable phases found present a rather high symmetry—i.e.,  $R3c$  or  $R\bar{3}c$  space groups—which allows us to use the unified structural description indicated in Table I.) For all the phases, we found oxygen-octahedron rotations (quantified by the  $g$ -type parameter  $z$  defined in Table I) as those occurring in the ferroelectric  $R3c$  phase of BFO at ambient pressure; our calculations show such rotations remain present under compression. The inversion-symmetry-breaking displacements in the

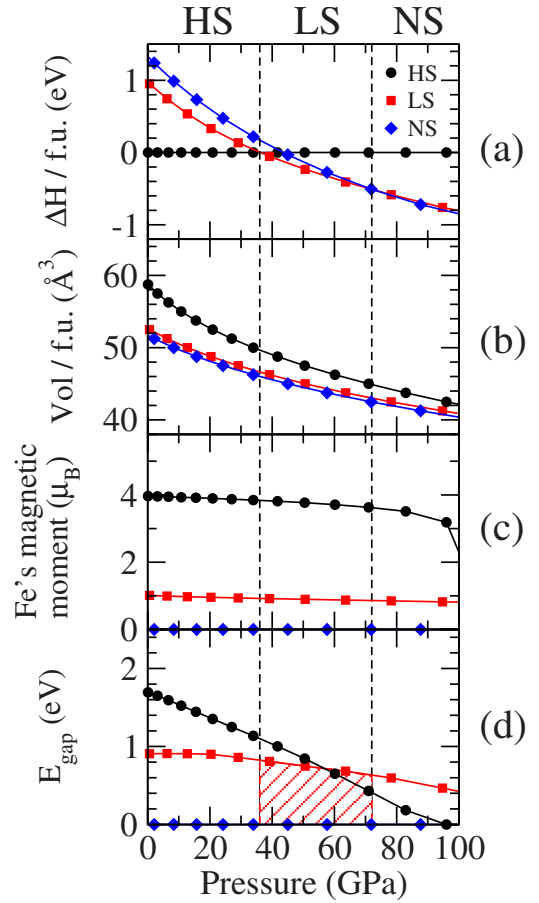


FIG. 2. (Color online). Pressure dependence of the (a) enthalpy, (b) volume, (c) Fe’s magnetic moment, (d) and electronic band gap of the HS, LS, and NS phases of BFO (see text). We give the results for all three phases in the whole pressure range, but note that each phase is stable only within one particular interval and metastable at other pressures. Dashed vertical lines mark the computed transition pressures. Panel (a): We take as the zero of enthalpy the pressure-dependent result for the HS phase. Panel (d): The highlighted area is suggestive of the subtleties pertaining to the value of  $E_{\text{gap}}$  in the LS phase (see text).

HS phase (quantified by the  $u$ -type parameters  $w$ ,  $x$ , and  $y$  defined in Table I) correspond to the usual ferroelectric distortion of BFO, which is dominated by the stereochemical activity of bismuth: in essence, the Bi atoms move along the  $[111]$  direction to approach the three O atoms forming a face of the neighboring oxygen octahedron. In the LS phase, though, we find that inversion symmetry is not broken (i.e.,  $w=x=y=0$ , corresponding to the  $R\bar{3}c$  space group), which reflects a change in bismuth’s coordination. As shown in Fig. 4, the LS phase presents  $\text{BiO}_3$  planar groups in which the three oxygen atoms binding with one Bi atom belong to three different  $\text{O}_6$  octahedra. Such planar groups are also present in the NS phase, but there they co-exist with a small  $u$ -type distortion ( $R3c$  space group).

These results clearly indicate that Bi coordination is the main factor controlling the occurrence of a  $u$ -type distortion in BFO under compression, in accordance with what is known about ferroelectricity in this material. Yet, one might

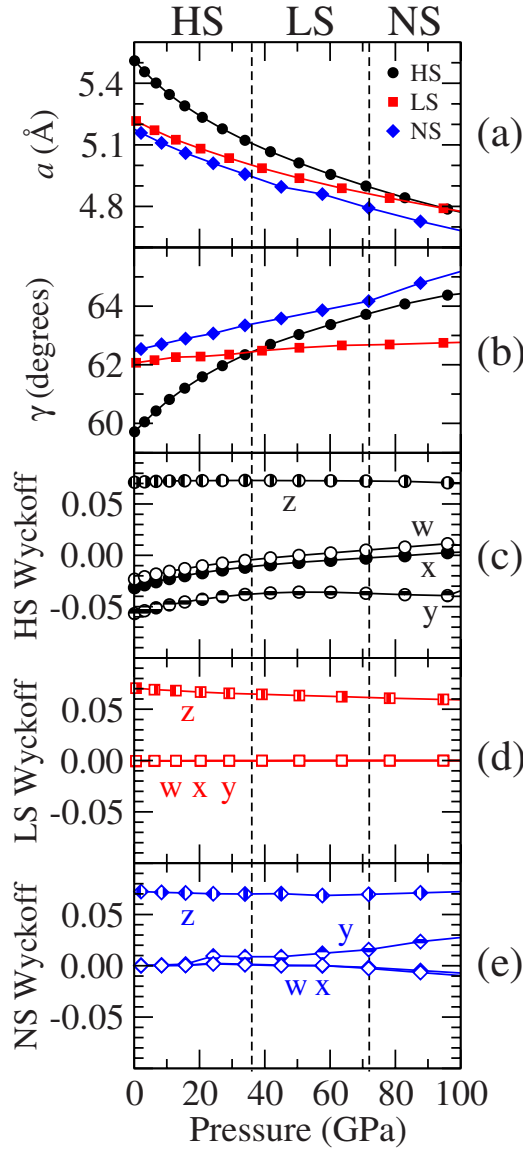


FIG. 3. (Color online). Pressure dependence of the structure of the HS, LS, and NS phases of BFO (see text). Shown are (a) the lattice parameter of the ten-atom unit cell, (b) the rhombohedral angle, and (c–e) the parameters associated to the occupied Wyckoff orbits as defined in Table I. We give the results for all three phases in the whole pressure range, but note that each phase is stable only within one particular interval and metastable at other pressures. Dashed vertical lines mark the computed transition pressures.

wonder why the  $\text{Fe}^{3+}$  cations present an off-centering  $u$ -type distortion in the HS and NS phases (at high pressures in the latter case), while such an off-centering is not observed in the LS case. We have not been able to find a simple explanation for this; as a matter of fact, it seems to us that the usual arguments from crystal-field theory might suggest to the contrary. We take this as an indication that one should be cautious when trying to interpret effects occurring at high pressures in terms of simple pictures that are known to apply essentially to materials at ambient conditions.

Thus, we found pressure favors two main modifications of the usual  $R3c$  phase, namely, a change in Bi coordination and a low- or null-spin configuration of the  $\text{Fe}^{3+}$  ions. We also

TABLE I. Structural parametrization for a unified description of all the phases here discussed (Ref. 17). Listed are the occupied Wyckoff orbits according to the rhombohedral setting of the  $R3c$  space group. The locations of the representative atoms are given as the sum of a reference position plus  $u$ -type (from *ungerade* or *odd under inversion*) and  $g$ -type (from *gerade* or *even under inversion*) distortions. The representative Bi is chosen to be at the origin. Whenever both  $u$ - and  $g$ -type distortions occur, we get the  $R3c$  space group; when only  $g$ -type ( $u$ -type) distortions exist, we obtain  $R\bar{3}c$  ( $R3m$ ); and when both  $g$ - and  $u$ -type displacements are null, we recover the ideal  $Pm\bar{3}m$  perovskite structure. In all cases, the ten-atom unit cell is fully specified by a single lattice parameter ( $a=b=c$ ) and the rhombohedral angle ( $\alpha=\beta=\gamma$ ).

Atom	Reference position	Distortions	
		$u$ type	$g$ type
Bi ( $2a$ )	(0,0,0)	$+(0,0,0)$	
Fe ( $2a$ )	(1/4,1/4,1/4)	$+(w,w,w)$	
O ( $6b$ )	(1/2,0,1/2)	$+(x,y,x)$	$+(z,0,-z)$

checked such variations can exist independently (e.g., LS  $\text{Fe}^{3+}$  can occur in absence of planar  $\text{BiO}_3$  groups), which gives rise to various metastable phases. Indeed, we obtained many metastable phases (not shown here) with different atomic and electronic structures, including the occurrence of intermediate-spin  $\text{Fe}^{3+}$ . We even found a mixed-spin phase, with one HS iron and one LS iron in our ten-atom cell, that becomes stable in the 35–37 GPa pressure range.

**B. Metallization at the HS-LS transition**

As expected, for the HS phase we obtained an AFM insulating ground state. The energy difference between the

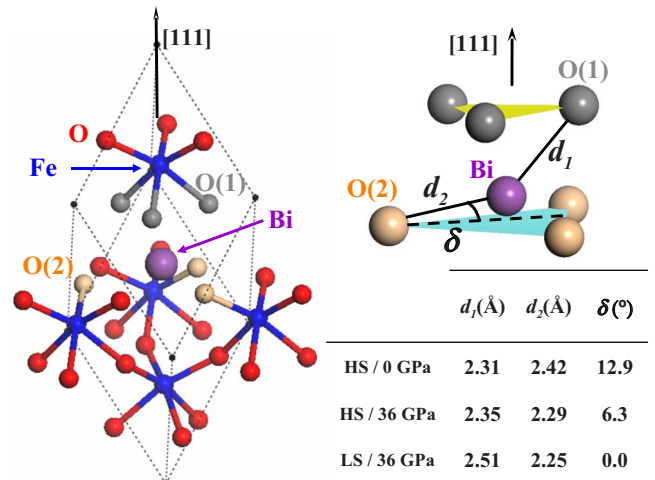


FIG. 4. (Color online). Left: surroundings of Bi in the BFO structure. The six nearest-neighboring oxygen atoms are split in two groups, denoted O(1) and O(2) and colored differently, each of which is composed of three symmetry-related atoms that form a plane perpendicular to the  $[111]$  direction. Right: Structural parameters relevant to the HS-LS transition.



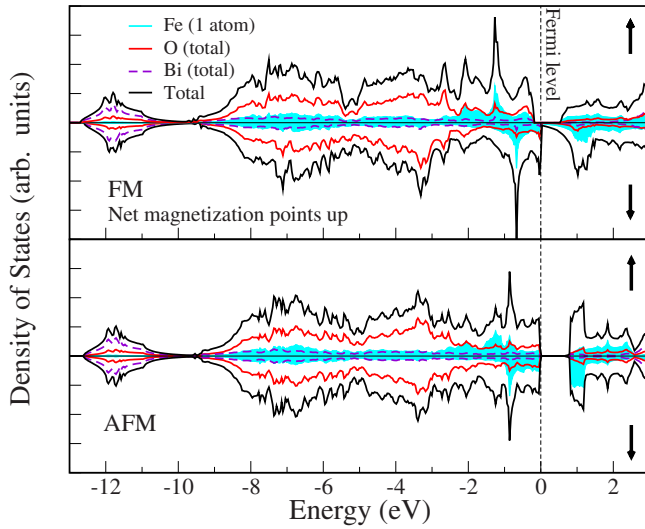


FIG. 5. (Color online). Electronic density of states of the FM and AFM configurations of the LS phase of BFO at 50 GPa. The shaded area indicates the result for one  $\text{Fe}^{3+}$  ion with its local magnetic moment pointing up.

AFM and ferromagnetic (FM) configurations varies from about 0.27 eV/f.u. at 0 GPa to about 0.65 eV/f.u. at 36 GPa, which is compatible with the experimentally observed high transition temperature ( $T_{\text{Neel}} \approx 643$  K at 0 GPa) and its increase with pressure.<sup>1</sup> As shown in Fig. 2(d), the HS phase is an insulator throughout its stability range, and its energy gap decreases with pressure.

According to our results, the properties of the LS phase are more complex. Throughout its stability range, the AFM and FM magnetic arrangements are nearly degenerate, never differing by more than 0.03 eV/f.u. (Moreover, the ground state shifts from AFM to FM as pressure increases.) This implies that the magnetic ordering temperature for the LS phase will be much (about ten times) smaller than that of the HS phase. We also found the electronic structure of the LS phase depends strongly on the magnetic order. Figure 5 shows illustrative results at 50 GPa: The AFM case presents a gap of about 0.8 eV, while for the FM order we get a half-metallic solution.

These results imply that if we were able to heat the LS phase up to room temperature ( $T_{\text{room}}$ ), we would obtain a paramagnetic state. Further, this magnetically disordered phase will probably appear as being metallic since the thermally averaged equilibrium state should present a significant electronic density of states at the Fermi level. Thus, our calculations suggest that, at  $T_{\text{room}}$ , BFO might undergo a pressure-driven HS-LS transition that brings about simultaneous structural, magnetic, and electronic (insulator-to-metal) transformations.

#### IV. DISCUSSION

The picture of the HS-LS transition that emerges from our simulations is essentially identical to the one suggested by Gavriluk *et al.*<sup>8</sup> to explain their observed pressure-driven transition. One should keep in mind, though, that the experi-

ments of Ref. 8 were performed at  $T_{\text{room}}$ ; thus, the identification between the experimental transition and our HS-LS transition relies on the assumption that our LS phase is the equilibrium state at  $T_{\text{room}}$ .

To resolve this issue, one would need to compute the temperature-pressure ( $T$ - $P$ ) phase diagram of BFO *ab initio*, which falls beyond the scope of this work. Yet, we can estimate the temperature stability range of the low- $T$  phases by calculating their enthalpy difference with the cubic phase, as such a quantity should be roughly proportional to the temperature at which the transition to the cubic phase occurs. At 0 GPa we obtained 0.88 eV/f.u. for the difference between the  $R3c$  HS phase and the lowest-lying cubic phase (which presents  $\text{Fe}^{3+}$  in a HS state), a large value consistent with the experimentally observed high transition temperature (1200 K).<sup>5,18</sup> This enthalpy difference decreases gently with pressure: For example, at 50 GPa, the  $R\bar{3}c$  LS phase and the lowest-lying cubic phase (which presents  $\text{Fe}^{3+}$  in a LS state) differ by about 0.60 eV/f.u. Hence, our calculations suggest that, within the stability range of the LS phase, the transition into a *LS cubic phase* will occur at temperatures well above  $T_{\text{room}}$  (roughly, in the 700–800 K range). Our results thus support the hypothesis of Gavriluk *et al.* that the metallic phase observed experimentally at high pressures and  $T_{\text{room}}$  contains LS  $\text{Fe}^{3+}$ .

We found additional support for this identification. The computed HS-LS transition pressure (about 36 GPa) agrees reasonably well with the observed one (40–50 GPa), and the wealth of competing (meta)stable phases that we found is consistent with the diffuseness of the experimental transition. Further, the results for  $V(P)$  in Fig. 2(b) are in good qualitative agreement with the experimental data, and the computed bulk modulus of the HS and LS phases are markedly different—the HS phase being significantly softer—as observed experimentally for the low- and high-pressure phases.<sup>19</sup> Finally, the pressure dependence of the enthalpy difference between the low- and high-pressure phases was experimentally determined to be 12 meV/GPa at the transition region, and we obtain about 15 meV/GPa.

It is not our purpose here to give a detailed electronic picture of the HS-LS transition that we found. Let us just note our results for BFO strongly resemble what occurs in hematite ( $\text{Fe}_2\text{O}_3$ ), which undergoes a HS-LS transition with accompanying metallization at 50 GPa.<sup>20–22</sup> Indeed, the conclusion of Ref. 22 that there is an enhancement of the metallic character of hematite's LS phase under pressure, driven by the broadening of the not-fully-occupied  $t_{2g}$  bands of  $\text{Fe}^{3+}$ , seems consistent with our findings. We should also note Gavriluk *et al.* recently described the pressure-induced metallization in BFO in terms of a Mott-Hubbard picture.<sup>9</sup> We have doubts about this interpretation: First-principles calculations show that BFO displays broad significantly hybridized valence bands (see Refs. 14 and 23 for the usual HS phase of BFO and Fig. 5 for our LS phase), which suggests it may not be adequate to place this material on the Mott-Hubbard side of the usual Zaanen-Sawatzky-Allen diagram.<sup>24</sup>

Our results allow us to discuss currently debated features of the  $T$ - $P$  phase diagram of BFO. Following the discovery

of the high-temperature metallic phase mentioned above,<sup>5</sup> which has the ideal cubic perovskite structure with a five-atom unit cell and  $Pm\bar{3}m$  space group, it has been proposed this phase might extend its stability range down to low temperatures and high pressures.<sup>1,25</sup> Our results suggest to the contrary. While restricted to a ten-atom cell, our simulations do include the ideal cubic perovskite as a possible solution, and show this phase does not become the ground state under compression. For pressures extending up to 100 GPa, we always observe symmetry-lowering distortions, associated to oxygen-octahedron tiltings and the stereochemical activity of Bi. This prediction is consistent with the experimental results of Graviliuk *et al.*<sup>8</sup> and Haumont *et al.*,<sup>26</sup> who observed a noncubic phase at high pressures and room temperature.

Finally, let us comment on the status of our *quantitative* results. As mentioned above, we repeated all our calculations for different values of the  $U$  parameter that defines the LDA+ $U$  functional. For the  $U$  values typically used in studies of BFO (Refs. 14, 15, and 27) and other oxides with Fe<sup>3+</sup> cations at the center of O<sub>6</sub> octahedra<sup>28</sup> (i.e., in the 3–4 eV range), the obtained qualitative results are identical. At the quantitative level, the main difference is a positive shift of the transition pressures as  $U$  increases. For example, for  $U = 4$  eV the HS-LS transition occurs at 42 GPa, as compared with 36 GPa for  $U = 3$  eV. The differences are greater for the LS-NS transition, which occurs at about 130 GPa for  $U = 4$  eV. This is not surprising, as a bigger value of  $U$  will tend to favor more insulating solutions. Hence, we think we can take our quantitative results as quite approximate in what regards the HS-LS transition and the properties of the HS and LS phases. The LS-NS transition pressure is, obviously, not well determined. We did not pursue a more detailed study of how our results depend on the type of LDA+ $U$  scheme or on the inclusion of a correction for the intra-atomic exchange ( $J$ ). Given the drastic simplifications made in this work as regards the simulated system (i.e., we restricted to a ten-atom unit cell), we thought it was not reasonable to insist further in the quantitative accuracy of the LDA+ $U$  scheme employed.

## V. SUMMARY AND CONCLUSIONS

We have identified the main structural, electronic, and magnetic effects that occur in BiFeO<sub>3</sub> under compression

and how they are connected. More precisely, our results reveal that pressure favors two main effects: (i) a change in the coordination of the Bi atoms, which tend to form planar BiO<sub>3</sub> groups, and (ii) a HS-LS crossover transition for Fe<sup>3+</sup> at pressures around 40 GPa. These are drastic transformations that involve relatively large energy scales. Thus, these predictions seem perfectly reliable, in spite of the approximations made in our theoretical study.

As regards the main magnetic and electronic properties of the LS phase, we find that (i) the magnetic interactions are relatively weak in that phase, which should result in a relatively low ordering temperature, and (ii) the electronic structure strongly depends on the magnetic order, which suggests that a (room-temperature) paramagnetic LS phase will be metallic. Our predicted HS-LS transition is thus consistent with the manifold (structural/magnetic/electronic) transformation observed experimentally by Gavriluk *et al.*,<sup>8</sup> and provides an explanation for it. In addition, we found a second transition, to a metallic phase with no localized magnetic moments, at very high pressures (above 70 GPa).

To conclude, let us stress that our investigation was by no means exhaustive and many issues remain open. For example, while our results strongly suggest that BFO will *not* present a cubic  $Pm\bar{3}m$  phase at high pressures, we cannot deduce from our calculations the space group of the high-pressure phases, as many possibilities (e.g., involving unit cells larger than the ten-atom one used in our simulations) have not been considered in this work. Similarly, the possibility that complex magnetic orders occur at high pressures has not been explored. Finally, quantitatively more accurate calculations of the transition pressures, and the properties of the high-pressure phases, would require the use of sophisticated first-principles techniques that can improve on our LDA+ $U$  results.

## ACKNOWLEDGMENTS

We acknowledge fruitful discussions with E. Canadell, G. Catalan, J. Kreisler, and J.F. Scott. This is work funded by MaCoMuFi (Grant No. STREP\_FP6-03321). It was also supported by CSIC (Grant No. PIE-200760I015), the Spanish Government (Grants No. FIS2006-12117-C04-01 and No. CSD2007-00041), the Catalan Government (Grant No. SGR2005-683), and FAME-NoE. We used the facilities provided by the CESGA supercomputing center.

<sup>1</sup>G. Catalan and J. F. Scott, Adv. Mater. (to be published).

<sup>2</sup>H. Béa, M. Bibes, F. Ott, B. Dupé, X.-H. Zhu, S. Petit, S. Fusil, C. Deranlot, K. Bouzehouane, and A. Barthélémy, Phys. Rev. Lett. **100**, 017204 (2008).

<sup>3</sup>H. W. Jang, S. H. Baek, D. Ortiz, C. M. Folkman, R. R. Das, Y. H. Chu, P. Shafer, J. X. Zhang, S. Choudhury, V. Vaithyanathan, Y. B. Chen, D. A. Felker, M. D. Biegalski, M. S. Rzchowski, X. Q. Pan, D. G. Schlom, L. Q. Chen, R. Ramesh, and C. B. Eom, Phys. Rev. Lett. **101**, 107602 (2008).

<sup>4</sup>P. Ravindran, R. Vidya, A. Kjekshus, H. Fjellvag, and O. Eriks-

son, Phys. Rev. B **74**, 224412 (2006).

<sup>5</sup>R. Palai, R. S. Katiyar, H. Schmid, P. Tissot, S. J. Clark, J. Robertson, S. A. T. Redfern, G. Catalan, and J. F. Scott, Phys. Rev. B **77**, 014110 (2008).

<sup>6</sup>J. Seidel, L. W. Martin, Q. He, Q. Zhan, Y.-H. Chu, A. Rother, M. E. Hawkrige, P. Maksymovych, P. Yu, M. Gajek, N. Balke, S. V. Kalinin, S. Gemming, F. Wang, G. Catalan, J. F. Scott, N. A. Spaldin, J. Orenstein, and R. Ramesh, Nat. Mats. (to be published).

<sup>7</sup>M. K. Singh, W. Prellier, M. P. Singh, R. S. Katiyar, and J. F.

- Scott, Phys. Rev. B **77**, 144403 (2008).
- <sup>8</sup>A. G. Gavriiliuk, V. V. Struzhkin, I. S. Lyubutin, M. Y. Hu, and H. K. Mao, JETP Lett. **82**, 224 (2005); A. G. Gavriiliuk, V. V. Struzhkin, I. S. Lyubutin, and I. A. Troyan, *ibid.* **86**, 197 (2007); A. G. Gavriiliuk, I. S. Lyubutin, and V. V. Struzhkin, *ibid.* **86**, 532 (2007).
- <sup>9</sup>A. G. Gavriiliuk, V. V. Struzhkin, I. S. Lyubutin, S. G. Ovchinnikov, M. Y. Hu, and P. Chow, Phys. Rev. B **77**, 155112 (2008).
- <sup>10</sup>J. P. Perdew and A. Zunger, Phys. Rev. B **23**, 5048 (1981); D. M. Ceperley and B. J. Alder, Phys. Rev. Lett. **45**, 566 (1980).
- <sup>11</sup>G. Kresse and J. Furthmüller, Phys. Rev. B **54**, 11169 (1996).
- <sup>12</sup>S. L. Dudarev, G. A. Botton, S. Y. Savrasov, C. J. Humphreys, and A. P. Sutton, Phys. Rev. B **57**, 1505 (1998).
- <sup>13</sup>P. E. Blochl, Phys. Rev. B **50**, 17953 (1994); G. Kresse and D. Joubert, *ibid.* **59**, 1758 (1999).
- <sup>14</sup>J. B. Neaton, C. Ederer, U. V. Waghmare, N. A. Spaldin, and K. M. Rabe, Phys. Rev. B **71**, 014113 (2005).
- <sup>15</sup>C. Ederer and N. A. Spaldin, Phys. Rev. B **71**, 060401(R) (2005).
- <sup>16</sup>M. Imada, A. Fujimori, and Y. Tokura, Rev. Mod. Phys. **70**, 1039 (1998).
- <sup>17</sup>M. I. Aroyo, J. M. Pérez-Mato, C. Capillas, E. Kroumova, S. Ivantchev, G. Madariaga, A. Kirov, and H. Wondratschek, Z. Kristallogr. **221**, 15 (2006).
- <sup>18</sup>The 1200 K transition to the cubic phase does *not* proceed from the  $R3c$  phase stable at low temperatures, but from an intermediate phase.<sup>5</sup> Yet, those 1200 K *measure* the strength of the symmetry-lowering distortions in BFO, and it seems reasonable to correlate this quantity with our computed enthalpy difference.
- <sup>19</sup>The computed bulk modulus ( $B_0$ ) increases strongly with pressure. For the HS phase we have  $B_0=130-300$  GPa within its stability range, and for the LS phase  $B_0=400-500$  GPa. Gavriiliuk *et al.* give a single value for their low- (76 GPa) and high-pressure (290 GPa) phases, which makes a comparison difficult. In fact, from the data in Ref. 8 we deduce  $B_0 \approx 180$  GPa for the low-pressure phase, a value much greater than the one (76 GPa) given by the authors themselves.
- <sup>20</sup>J. Badro, G. Fiquet, V. V. Struzhkin, M. Somayazulu, H.-K. Mao, G. Shen, and T. Le Bihan, Phys. Rev. Lett. **89**, 205504 (2002).
- <sup>21</sup>G. Rollmann, A. Rohrbach, P. Entel, and J. Hafner, Phys. Rev. B **69**, 165107 (2004).
- <sup>22</sup>A. V. Kozhevnikov, A. V. Lukoyanov, V. I. Anisimov, and M. A. Korotin, J. Exp. Theor. Phys. **105**, 1035 (2007).
- <sup>23</sup>S. J. Clark and J. Robertson, Appl. Phys. Lett. **90**, 132903 (2007).
- <sup>24</sup>J. Zaanen, G. A. Sawatzky, and J. W. Allen, Phys. Rev. Lett. **55**, 418 (1985).
- <sup>25</sup>J. F. Scott, R. Palai, A. Kumar, M. K. Singh, N. M. Murari, N. K. Karan, and R. S. Katiyar, J. Am. Ceram. Soc. **91**, 1762 (2008).
- <sup>26</sup>R. Haumont, P. Bouvier, A. Pashkin, K. Rabia, S. Frank, B. Dkhil, W. A. Crichton, C. A. Kuntscher, and J. Kreisel, arXiv:0811.0047 (unpublished).
- <sup>27</sup>I. A. Kornev, S. Lisenkov, R. Haumont, B. Dkhil, and L. Bellaiche, Phys. Rev. Lett. **99**, 227602 (2007).
- <sup>28</sup>The case of hematite is specially reassuring for us. As mentioned in Sec. IV, pressure-driven effects in  $\text{Fe}_2\text{O}_3$  are very similar to the ones we found in BFO, and are seemingly well established both experimentally<sup>20</sup> and theoretically. In particular, LDA+ $U$  results for hematite<sup>21</sup> are in qualitative agreement with recent dynamical mean-field theory calculations,<sup>22</sup> which supports the adequacy of the LDA+ $U$  approach here adopted.